Applied Catalysis B: Environmental 182 (2016) 392–404

Contents lists available at ScienceDirect

Applied Catalysis B: Environmental

journal homepage: www.elsevier.com/locate/apcatb

Visible light-triggered vanadium-substituted molybdophosphoric acids to catalyze liquid phase oxygenation of cyclohexane to KA oil by nitrous oxide

Jialuo She[a], Zaihui Fu[b,*], Jianwei Li[a,**], Bin Zeng[b], Senpei Tang[b], Wenfeng Wu[b], Haihong Zhao[b], Dulin Yin[b], Steven Robert Kirk[b]

[a] State Key Laboratory of Chemical Resource Engineering, Bejing University of Chemical Technology, Beijing 100029, PR China
[b] National & Local United Engineering Laboratory for New Petrochemical Materials & Fine Utilization of Resources, Key Laboratory of Resource Fine-Processing and Advanced Materials of Hunan Province and Key Laboratory of Chemical Biology and Traditional Chinese Medicine Research (Ministry of Education of China), College of Chemistry and Chemical Engineering, Hunan Normal University, Changsha 410081, PR China

ARTICLE INFO

Article history:
Received 10 March 2015
Received in revised form 19 August 2015
Accepted 26 September 2015
Available online 30 September 2015

Keywords:
Nitrous oxide
Vanadium-substituted heteropolyacid
Donor–acceptor
Photocatalytic oxidation
Cyclohexane

ABSTRACT

The development of a mild and highly efficient process for utilization of nitrous oxide (N_2O) as a green oxidant has very important academic and applied values in the synthesis of oxygenated products. This paper first discloses that a series of vanadium-substituted molybdophosphoric acids ($PMo_{12-n}V_n$, $n = 1–3$), assisted by HCl aqueous solution, can efficiently catalyze the visible light-driven liquid phase oxygenation of cyclohexane by N_2O in acetonitrile (MeCN), providing ca. 26.2% cyclohexane conversion and 90.2% selectivity for cyclohexanol and cyclohexanone (KA oil) under optimized conditions, along with a small quantity of chlorination. Among the catalysts examined, $PMo_{10}V_2$ and especially PMo_9V_3 showed a higher activity for this photocatalytic oxygenation than $PMo_{11}V$. Furthermore, the amount of water added strongly influenced this HCl-promoted photocatalysis oxygenation. The selectivity of cyclohexanone was continuously and significantly improved from 21.8 to 82.7% with increasing water amount from 0 to 0.15 mL, but the conversion of cyclohexane obviously decreased when the amount of water added was higher than 0.12 mL. The promoting effect of HCl on the present photocatalysis reaction is probably due to the fact that the donor–acceptor (D–A) adduct between HCl and $PMo_{12-n}V_n$ can be excited by visible light to achieve its intra-molecular electron transfer from Cl^- to $PMo_{12-n}V_n$ anions, which leads to the generation of $Cl^•$ radicals and the reduction of catalysts. The subsequent reactions initiated by the $Cl^•$ radicals result in the oxygenation of cyclohexane by N_2O to KA oil and the regeneration of catalysts, as supported by UV–vis spectral and cyclic voltammetric measurements.

1. Introduction

Nitrous oxide (N_2O), with its strong greenhouse effect and long residence time in the lower layers of the atmosphere, gives rise to serious global environmental problems [1,2]. N_2O generated by anthropogenic activities is considered as the main factor leading to the imbalance of its concentration in the atmosphere [2]. Notably, the predominant industrial process to produce adipic acid (AA), an important building block for varieties of fine chemicals [3], is still oxidation of a mixture of cyclohexanone and cyclohexanol (KA oil for short) by an excess use of HNO_3 in the presence of copper(II) and ammonium metavanadate catalysts [2,3]. This process inevitably produces considerable amount of N_2O accounting for nearly 8% of total anthropogenic emissions [1,3]. Some efficient processes for cutting down the amount of N_2O exhausted into the atmosphere, such as catalytic decomposition [4–8], selective catalytic reduction (SCR) [9–12] or utilization as an oxidant in the synthesis of fine chemicals [13–15], have been developed by many scholars worldwide, but greater efforts are under way to develop more practical and efficient catalysis technologies to reduce the N_2O emissions. The synthesis technology for KA oil is another problem encountered by the production of AA. There have developed some efficient catalytic processes for selective oxygenation of cyclohexane to KA oil by dioxygen (O_2) under heating or light illumination [16–18]. The current industrial process for producing KA oil, however, mainly relies on the cobalt-catalyzed oxidation

* Corresponding author. Fax: +86 731 88872531.
** Corresponding author. Fax: +86 10 64436787.
E-mail addresses: fzhhnnu@126.com (Z. Fu), lijw@mail.buct.edu.cn (J. Li).

http://dx.doi.org/10.1016/j.apcatb.2015.09.048
0926-3373/

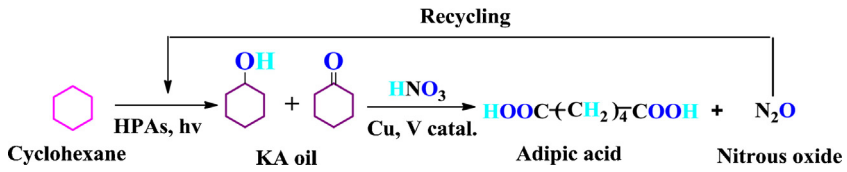

Scheme 1. Simplified reaction scheme of the mild and green process for adipic acid production by photocatalytic oxidation of cyclohexane by recycling N_2O and then catalytic oxidation of the resulting KA oil with nitric acid.

of cyclohexane with air under harsh conditions [19], which should restrain conversion (lower than 8%) to get high selective KA oil [20].

N_2O has advantages of high oxygen content (36 wt%), thermodynamic spontaneity and environmentally benign by-product (N_2) in the oxidation of various organic substrates, so that it is regarded as a potential oxidant [1,21]. Furthermore, N_2O is more conductive to selective oxidation than traditional air or O_2 [1,21]. Considerable progress, therefore, has been achieved in catalytic oxygenations based on using N_2O as an oxidant, which includes gaseous or liquid phase oxidation of aliphatic and aromatic hydrocarbons [21–30], alkenes [31–34], alcohols [23] and phosphines [35] under heterogeneous or homogeneous conditions. In these catalytic transformations, the use of a N_2O-containing stream for hydroxylation of benzene to phenol catalyzed by Fe-ZSM-5 zeolite [24–28] is highly appreciated because its product phenol can be hydrogenated into cyclohexanol to complete N_2O cycle [29]. The deactivation of catalyst and the excess use of benzene in this process, however, elevate operating costs [29,30]. N_2O can react with some special reagents under mild liquid-phase conditions [36,37]; however, it usually needs to be activated by high temperature (150–500 °C) and often elevated pressure to efficiently participate in various catalytic oxidations under gaseous or liquid phase conditions [21], which is due to its inertness in kinetics [33,38] and weak coordination ability to the transition metals [39]. Consequently, it is highly desirable to develop a milder and more efficient catalysis technology aimed at the selective oxidation of inactive organic compounds by N_2O to synthesize various oxygenated products.

Heteropolyacids (HPAs), especially the Keggin-type, have been extensively used as promising catalysts for various oxygenations with hydrogen peroxide [40] or O_2 [40–42] as an oxidant, as well as photo-oxidative degradation of various organic pollutants in water [43]. To the best of our knowledge, however, the visible light-triggered selective oxygenation of cyclohexane to KA oil catalyzed by HPAs has rarely been reported so far. Developing such a new photocatalytic technology to obtain cyclohexane-derived KA oil by using N_2O under mild conditions is of both environmental and economic significances in the recycling of N_2O and the production of AA (see Scheme 1). Moreover, the economical efficiency of this process is better than traditional hydroxylation of benzene by N_2O since the new process can avoid hydroprocessing to yield KA oil. Herein, we report initial results obtained from using the vanadium-substituted molybdophosphoric acids to photocatalyze selective oxidation of cyclohexane to KA oil by N_2O with the participation of HCl aqueous solution.

2. Experimental

2.1. Materials and reagents

Materials and reagents used in this study were of analytical grade. They included cyclohexane, *n*-hexanol, acetonitrile (MeCN), diethyl ether, $Na_2HPO_4{\cdot}12H_2O$, $Na_2MoO_4{\cdot}2H_2O$, V_2O_5, Na_2CO_3, LiCl, concentrated HCl and H_2SO_4, 12-molybdophosphoric acid (PMo_{12}), N_2O (99.9%). Distilled water was used throughout this experiment.

Table 1
The P, Mo and V contents of V(V)-substituted molybdophosphoric acids measured by an ICP method.

Entry	Sample	P (wt/%)	V (wt/%)	Mo (wt/%)	Actual formula
1	$PMo_{11}V_1$	1.596	2.314	55.650	$PMo_{11.26}V_{0.88}$
2	$PMo_{10}V_2$	1.817	6.322	57.050	$PMo_{10.14}V_{2.12}$
3	PMo_9V_3	1.718	8.404	48.350	$PMo_{9.09}V_{2.97}$

2.2. Preparation of V(V)-substituted molybdophosphoric acids

Referring to the method reported in the literature [44], a series of V(V)-substituted molybdophosphoric heteropolyacids (HPAs, $PMo_{12-n}V_n$, $n = 1-3$) were prepared using $Na_2HPO_4{\cdot}12H_2O$, $Na_2MoO_4{\cdot}2H_2O$ and V_2O_5 as P, Mo and V sources, respectively. The preparation process of a typical PMo_9V_3 acid is described as follows: $Na_2HPO_4{\cdot}12H_2O$ (1.79 g, 5 mmol) and $Na_2MoO_4{\cdot}2H_2O$ (10.89 g, 45 mmol) were dissolved in 50.0 mL of distilled water and then heated to 110 °C for 30 min to obtain a solution, designated as "A". V_2O_5 (1.59 g, 8.75 mmol) was dissolved in 10.0 mL of Na_2CO_3 solution (1.0 M) to form the solution "B". The solution "B" was added to the solution "A" under magnetic stirring, followed by heating at 90 °C for 30 min. After reaction, the obtained solution was treated with H_2SO_4 solution (9.0 M, dropwise and with stirring) until the pH was 2.0 and then cooled to room temperature. This step was followed by introduction of diethyl ether (30 mL) and then slowly dropping H_2SO_4 (9.0 M) until this dark red solution became pale yellow. The resulting deep red oil in the bottom of separating funnel was evaporated to remove diethyl ether under vacuum. Finally, the crude product $H_6PMo_9V_3O_{40}$ was dissolved with suitable amount of water and then recrystallized as crystalline, deep-red solid (with yield, higher than 80%). Similar procedures were used to prepare $PMo_{11}V$ and $PMo_{10}V_2$ acids through adjusting the Mo/V mole ratio of $Na_2MoO_4{\cdot}2H_2O$ to V_2O_5 to be 11:1 and 10:2.5, respectively. The P, Mo and V contents of three $PMo_{12-n}V_n$ acids measured on a PerkinElmer Optima 5300DV-ICP are listed in Table 1. It is seen from Table 1 that the actual measured molecular formulas of these V(V)-substituted HPAs are basically accordant with their theoretical ones.

2.3. Characterizations of HPAs

2.3.1. Spectral characterizations

The samples HPAs, unless otherwise specified, were dried in a vacuum oven at 50 °C for 3 h before characterizations. Liquid UV–vis spectra of the HPAs in MeCN were recorded from 200 to 800 nm on a Shimadzu UV-2450 spectrophotometer and their transmission FT-IR spectra were measured from 400 to 4000 cm^{-1} on a Nicolet Nexus 510 P FT-IR spectroscopy using a KBr disc. Powder X-ray diffraction (XRD) analyses of the HPAs were conducted on a Rigaku 2550 X-ray diffractometer using Cu Kα radiation ($\lambda = 0.15406$ nm) and a graphite monochromator, operated at a voltage of 40 kV, a current of 250 mA and a slit width of 0.15 mm. XRD patterns were collected in the angular range of 5–50° with a scanning rate 2°/min. X-ray photoelectron spectroscopy (XPS) measurements were carried out on a ESCALAB 250Xi spectrometer. The experiments were performed using a monochromatic Al Kα X-ray

source ($h\nu$ = 1486.6 eV, beam diameter, 650 μm) at 200 W with a pass energy of 30 eV (0.05 eV/step) for high resolution spectra and a pass energy of 100 eV (1 eV/step) for the survey spectrum. The base pressure in the analysis chamber was below 1×10^{-9} mbar. To define binding energies (BEs) of different elements, the C 1s line of contaminant carbon at 284.8 eV was taken as a reference.

2.3.2. Cyclic voltammetric measurements

Cyclic voltammetric (CV) measurements of the HPAs were carried out on a three-electrode configuration with an CHI660C electrochemical workstation. The working, counter and reference electrodes used in CV experiments were a glassy carbon electrode (GCE, 3 mm diameter disk), carbon electrode and KCl-saturated calomel electrode (SCE), respectively. All the electrochemical experiments were carried out at room temperature (20 °C). All potentials here were reported at scan rate of 100 mV/s versus the SCE.

2.4. Procedure of photocatalytic oxygenation

The photo-oxygenation of cyclohexane catalyzed by HPAs in MeCN was carried out under non-current N_2O atmosphere (1 atm) in a sealed photo-reactor equipped with a water-cooled condenser. A tungsten-bromine lamp (35 W) equipped with an UV light filter was immersed in the acetonitrile (5 mL) solution containing cyclohexane (1 mmol) and HPAs (0.01 mmol). The gasbag (40 L) storing N_2O was connected to the photo-reactor. Before photoreaction, the N_2O was continuously fed into the lower portion of the reactor for 40 s in order to remove the air inside the reactor. The following reaction operating procedures and the analytical method of oxidative products can be found in our previously published work [45].

3. Results and discussion

3.1. Characterizations of HPAs

Fig. 1 provides FT-IR spectra of the HPAs. Some characteristic adsorption peaks due to the Keggin structure in the range of 1100–700 cm^{-1} were observed clearly in the FT-IR spectrum of PMo_{12} acid. These characteristic peaks, at 1064.6, 962.4, 867.9 and 794.6 cm^{-1}, are assigned to asymmetric stretching vibrations of P—O_a (O_a: oxygen located at PO_4 tetrahedron), Mo = O_d (O_d: terminal oxygen), Mo–O_b–Mo (O_b: corner-sharing bridged oxygen) and Mo–O_c–Mo (O_c: edge-sharing bridged oxygen), respectively [44,46]. Also, the characteristic peaks above-mentioned could be found in the FT-IR spectra of three $PMo_{12-n}V_n$ acids, but all showed different degrees of red-shift when V atoms were incorporated into HPAs (see Supplementary data, Table S1). The P–O_a and Mo=O_d vibration frequencies respectively followed a descending order: 1060.7 and 960.4 cm^{-1} (for $PMo_{11}V$) >1058.8 and 958.5 cm^{-1} (for $PMo_{10}V_2$) > 1054.9 and 956.6 cm^{-1} (for PMo_9V_3). In addition, the peak attributed to the asymmetric vibration of P—O_a became asymmetric and its splitting trend near 1080 cm^{-1} could be noticed in the FT-IR spectra of three $PMo_{12-n}V_n$ acids. These spectral changes should originate from that incorporating vanadium into the primary structure of Keggin anion leads to reduced structural symmetry [47,48]. Notably, the spectra of three $PMo_{12-n}V_n$ acids did not clearly exhibit a shoulder peak at 1035 cm^{-1} attributed to the isolated vanadium oxide ($V^{5+}O_x$) [49], indicating that most of

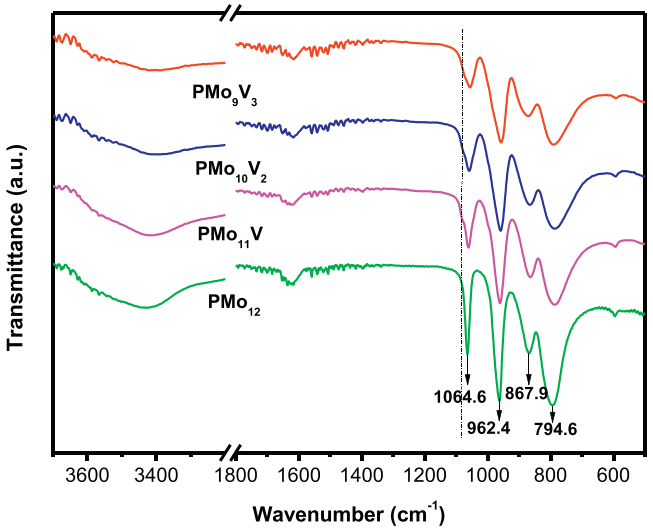

Fig. 1. FT-IR spectra (3700–500 cm^{-1}) of PMo_{12} and $PMo_{12-n}V_n$ heteropolyacids.

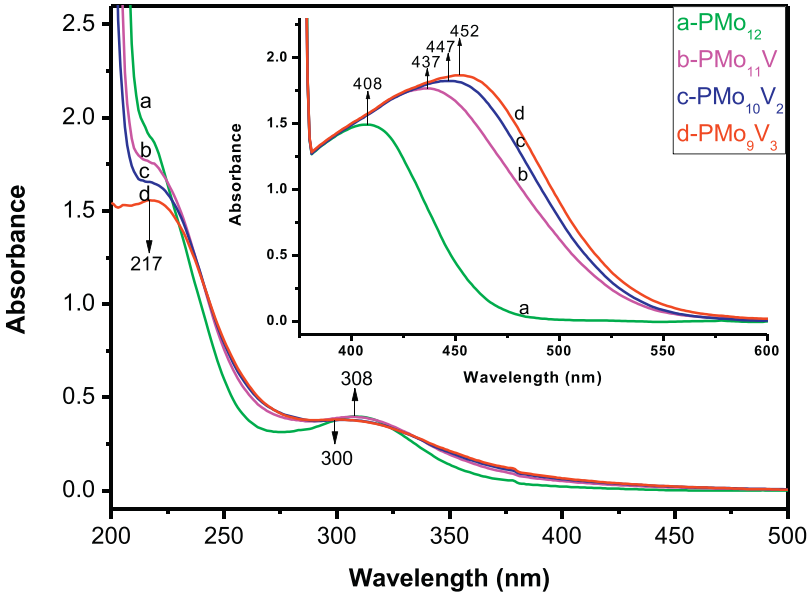

Fig. 2. UV–vis spectra (200–500 nm) of PMo_{12} and $PMo_{12-n}V_n$ heteropolyacids in MeCN (2.00×10^{-5} M). Inset are the visible spectra (380–600 nm) of these heteropolyacids with a higher concentration (2.00×10^{-3} M).

the vanadium atoms in these HPAs have been incorporated into the primary structure of Keggin anions.

Fig. 2 shows UV–vis spectra of the above-mentioned HPAs in MeCN. Two characteristic adsorption bands in the region of 200–310 nm appeared in the UV–vis spectrum of PMo_{12} acid (Fig. 2a), in accordance with previous report [50]. The strong absorption band at λ near 220 nm should originate from oxygen to molybdenum charge transfer (LMCT) of the Mo=O_d bonds and another weak LMCT band at λ = 308 nm should originate from the Mo—$O_{b(c)}$ bonds in the Keggin structure [50,51]. Also, three $PMo_{12-n}V_n$ acids exhibited the two LMCT bands described above in their UV–vis spectra, indicating that they have a similar Keggin structure to the parent PMo_{12}. Notably, a blue-shift and a broadening of the Keggin structural band were noticed in their UV–vis spectra (Fig. 2b–d). This further supports the assertion that the incorporation of vanadium into the primary structure of HPAs results in reduced structural symmetry [51]. Moreover, the Keggin structural band centered around 300–310 nm in these HPAs exhibited an absorption edge prolonged to the visible region of 380–500 nm and its absorbance in this visible region was strengthened in the $PMo_{12-n}V_n$ acids. Interestingly, when the concentration of these HPAs was increased by 100 fold, an absorption band in 380–500 nm was respectively noticed in their spectra (see inset in Fig. 2), which is likely due to a d–d transition of the coordinated metal Mo or V atoms [52]. This band was continuously and significantly strengthened and shifted to a low energy region upon increasing the degree of substitution of V atoms into HPAs.

The PMo_{12} and PMo_9V_3 acids were pretreated in a vacuum oven at 100 °C until no significant pressure (about 1 mbar) change was noticed. Then the samples were characterized by XPS. The signals of three elements were studied in detail: P 2p, Mo 3d and V 2p (Fig. 3). As shown in Fig. 3(a_1), the XPS spectrum of PMo_{12} acid showed only one P 2p peak at 134.27 eV, which is assigned to the P^{5+} ion in phosphates [53,54]. This seems to indicate that there is only one kind of P^{5+} ion in PMo_{12} acid. This value was lower than that of P_2O_5 (135 eV [55]), indicating that the coordinated Mo atoms can transfer their electrons toward the centered phosphorus atom because of their lower electronegativity. Fig. 3 (b_1) shows that the XPS peaks of Mo $3d_{5/2}$ and Mo $3d_{3/2}$ over PMo_{12} acid appeared at 233.30 and 236.45 eV, respectively, which are characteristic of Mo^{6+} in oxides [54]. The binding energy (BE) attributed to the main peak Mo $3d_{5/2}$ was higher than that of MoO_3 (232.65 eV [55]), further supporting that the electron transfer process above-described. In comparison with the PMo_{12} acid, the BEs for P 2p, Mo $3d_{5/2}$ and Mo $3d_{3/2}$, which appeared at 134.05 eV, 233.15 and 236.29 eV, respectively, exhibited different degree of decline in the XPS spectra of PMo_9V_3 acid (Fig. 3 (a_2) and (b_2)). Fig. 3 (c) shows that the XPS peaks of V $2p_{3/2}$ and V $2p_{1/2}$ over PMo_9V_3 acid were located at 517.97 and 525.30 eV,

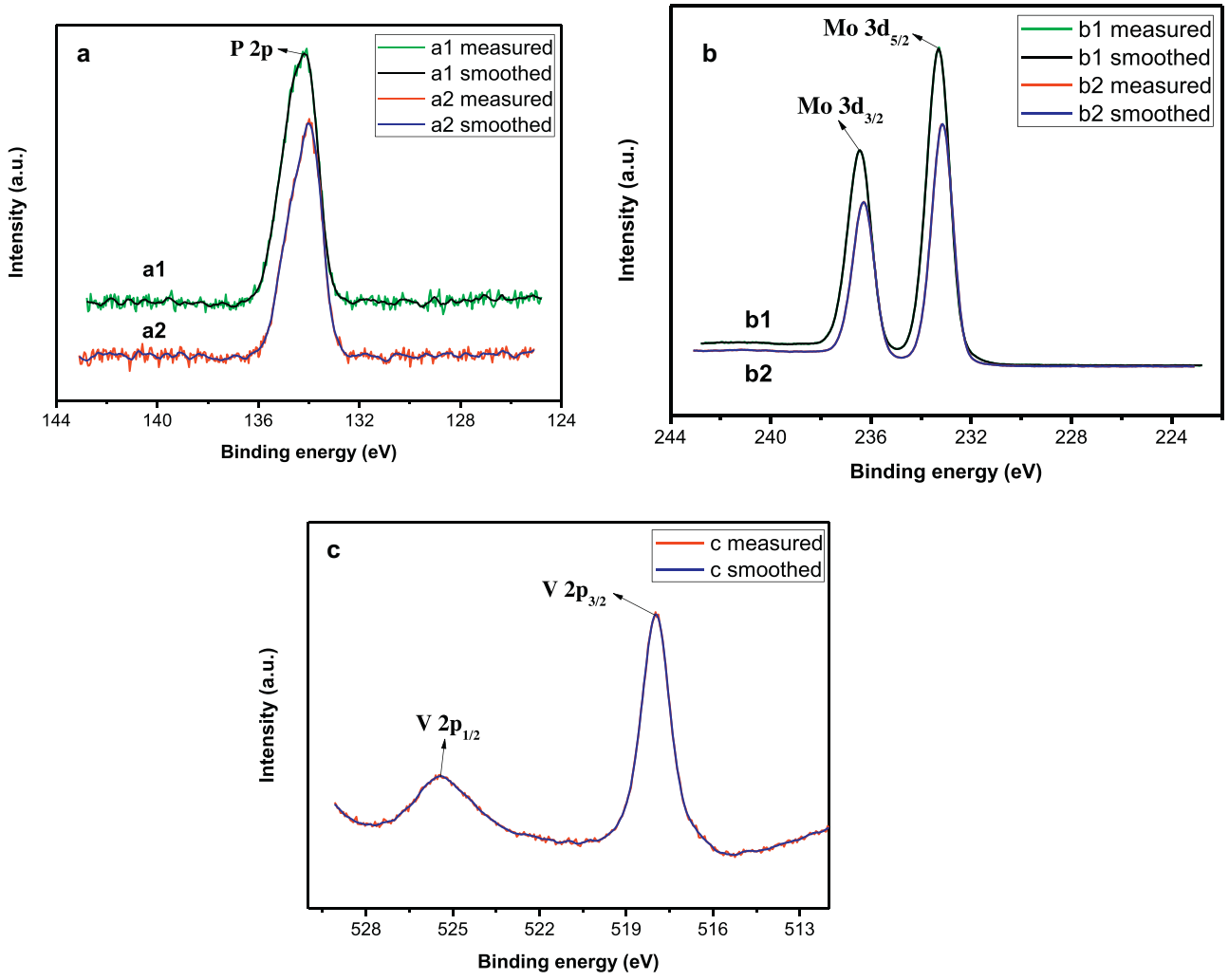

Fig. 3. XPS spectra for P 2p (a), Mo 3d (b) and V 2p (c) of PMo_{12} and PMo_9V_3 heteropolyacids.

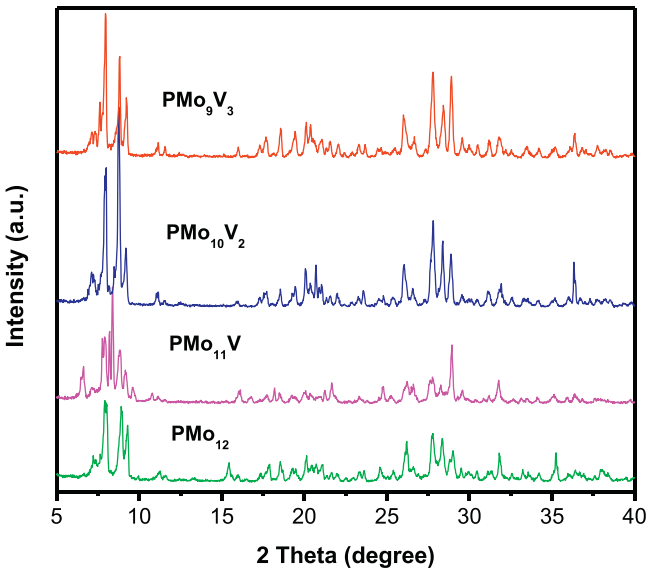

Fig. 4. XRD patterns of PMo_{12} and $PMo_{12-n}V_n$ heteropolyacids.

respectively, which can correspond to V^{5+} in oxides [54,56]. The BE of main peak V $2p_{3/2}$ was higher than that of V_2O_5 (517.45 eV [55]). These findings support that the electron transfer or delocalization from V atom toward Mo and P atoms exists in PMo_9V_3 acid.

Crystalline phases of the HPAs were studied on a powder XRD. As shown in Fig. 4, some characteristic XRD peaks at the 2θ values of 7.92, 8.90, 9.30, 27.78, 28.36 and 29.00° were observed in the XRD pattern of PMo_{12} and they are attributed to the typical Keggin structure anion [50,52]. Also, these characteristic peaks appeared in the XRD patterns of three V-substituted HPAs and their positions were only slightly influenced by the incorporation of vanadium (Fig. 4 and Supplementary Data, Table S2), illustrating that the Keggin structure is well preserved after incorporating vanadium into the primary structure of heteropoly anion. Notably, drying these samples under mild temperature, as reported in literature [50,57], easily brought out new XRD peaks in the two regions (15–27° and 29–40°). This is likely due to the crystalline phase transition of HPAs caused by the loss and the reorganization of crystalline water [50,54,57].

3.2. Photocatalytic oxidation performance of V(V)-substituted HPAs

Table 2 summarizes the data of the HPAs-catalyzed oxygenation of cyclohexane by N_2O in MeCN containing different additives under visible light irradiation. As shown in Table 2, this photo-oxygenation in a pure MeCN medium did not occur on the parent PMo_{12} acid (Entry 1), but it could be catalyzed by three $PMo_{12-n}V_n$ acids, achieving lower than 0.7% cylcohexane conversion with cyclohexanol and cyclohexanone as the main oxygenated products (Entries 2–4). These findings indicate that the direct activation of substrate cyclohexane or N_2O can not occur on PMo_{12} under aforementioned conditions and these processes can hardly proceed even if the V(V)-substituted HPAs acids, with stronger oxidative capacity, were used as catalysts. Entry 5 shows that the addition of water to the PMo_9V_3 photocatalysis system did not improve its photocatalytic activity. Interestingly, a suitable amount of HCl aqueous solution (12 M, 0.1 mL) was found to significantly promote the present photo-oxygenation catalyzed by $PMo_{12-n}V_n$ acids and its promoting effect followed an ascending sequence of $PMo_{11}V$ (15.5%) <$PMo_{10}V_2$ (19.7%) <PMo_9V_3 (20.9%). In addition, it could afford a higher selectivity for cyclohexanone (Entries 7–9, 70.1–72.4%), along with a small amount of chlorination. The HCl aqueous solution did not, however, show any promoting effect on the PMo_{12}-catalyzed photo-oxygenation (Entry 6). Entries 10 and 11 demonstrate that the PMo_9V_3-catalyzed oxygenation of cyclohexane by N_2O did not happen without irradiation regardless of whether the additive HCl aqueous solution was present or absent, indicating that the present catalysis oxidation is indeed driven by visible light illumination. Entry 12 shows that the HCl aqueous solution itself did not initiate this photo-oxygenation in the absence of HPAs. Entries 13 and 14 illustrate that the other two additives H_2SO_4 aqueous solution and LiCl were inefficient to promote the PMo_9V_3-photocatalyzed oxygenation for lack of either Cl^- or H^+. These findings likely imply that only the additive HCl aqueous solution can be oxidized by the visible light-excited $PMo_{12-n}V_n$ acids to generate a chlorine radical ($Cl^\bullet$), and then the latter easily

Table 2
Oxygenation of cyclohexane with N_2O catalyzed by $PMo_{12-n}V_n$ acids in the presence of various additives under visible light illumination.[a]

Entry	Catalyst	Additive (mmol)	Water/mL	Conv./%	Selectivity of products[b] (%)		
					Cyclohexanone	Cyclohexanol	Chlorocyclohexane
1	PMo_{12}	–	–	0	–	–	–
2	$PMo_{11}V$	–	–	0.3	48.0	52.0	–
3	$PMo_{10}V_2$	–	–	0.6	33.1	66.9	–
4	PMo_9V_3	–	–	0.7	31.4	68.6	–
5	PMo_9V_3	–	0.1	0.4	40.5	59.5	–
6[c]	PMo_{12}	HCl (1.2)	0.1	0	–	–	–
7[c]	$PMo_{11}V$	HCl (1.2)	0.1	15.5	72.4	22.4	5.2
8[c]	$PMo_{10}V_2$	HCl (1.2)	0.1	19.7	70.1	23.3	6.6
9[c]	PMo_9V_3	HCl (1.2)	0.1	20.9	70.7	21.6	7.7
10[d]	PMo_9V_3	–	–	0	–	–	–
11[c,d]	PMo_9V_3	HCl (1.2)	0.1	0	–	–	–
12[c,e]	–	HCl (1.2)	0.1	0	–	–	–
13[f]	PMo_9V_3	H_2SO_4(0.6)	0.1	0.3	100	–	–
14	PMo_9V_3	LiCl (1.2)	0.1	1.0	38.5	60.5	1.0
15[g]	PMo_9V_3	–	–	2.1	100		–

[a] Cyclohexane (1.0 mmol), catalyst (0.01 mmol), MeCN (5.0–5.1 mL), N_2O (1 atm), temperature (30–35 °C), time (12 h), using 35 W of tungsten–bromine lamp as visible light source.
[b] Product selectivity = (the content of this product/$\sum$content (mmol) of each product) × 100%.
[c] Adding 12 M HCl aqueous solution (0.1 mL).
[d] Heating (35 °C) in the dark.
[e] Without catalyst.
[f] Adding 6.0 M H_2SO_4 aqueous solution (0.1 mL).
[g] Using cyclohexanol (1 mmol) as a substrate.

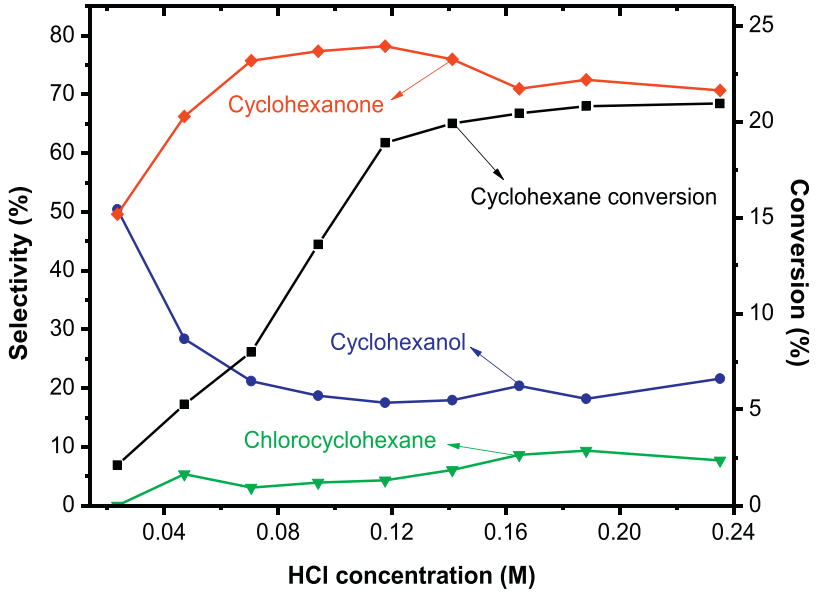

Fig. 5. Effect of HCl concentration on the PMo_9V_3 (0.01 mmol, 1.96×10^{-3} M)-photocatalyzed oxidation of cyclohexane (1 mmol) by N_2O in MeCN (5.0 mL) and water (0.1 mL) under visible light irradiation (12 h).

initiates the present photoreaction. Moreover, photo-catalysis efficiency is likely dependant on the oxidative capacity of $PMo_{12-n}V_n$ acids.

3.3. Effect of various process variables

In the following experiments, the effects of HCl and catalyst concentration, irradiation time and water amount on the photocatalytic oxidation of cyclohexane by N_2O in MeCN under visible light irradiation were further examined using the best PMo_9V_3 acid as a catalyst. The results are shown in Figs. 5–8 respectively. Fig. 5 shows that when the concentration of HCl in MeCN was between 0.024 and 0.120 M, the curve of cyclohexane conversion linearly ascended with increasing HCl concentration and the selectivity for cyclohexanone was rapidly improved from 49.6 to 78.2%, with a concomitant decrease of cyclohexanol selectivity. On further increasing HCl concentration, the conversion increased very slowly and cyclohexanone selectivity slightly decreased. Chlorocyclohexane selectivity gradually increased with increasing HCl concentration. These findings indicate that the reaction pathway to generate cyclohexanone is likely controlled by HCl concentration. Fig. 6 illustrates that when the concentration of catalyst (relative to substrate) was between 0.1 and 1.0 mol%, cyclohexane conversion gradually increased from 14.9 to 20.9% with increasing the concentration. After that, the conversion hardly varied with further increasing catalyst concentration. Cyclohexanone selectivity continuously and slowly decreased with catalyst concentration, along with an increase of cyclohexanol. Fig. 7 shows that when irradiation time was between 1 and 10 h, the conversion of cyclohexane continuously and significantly increased from 1.0 to 20.4% with increasing time. After 10 h, it slowly increased with time and eventually achieved 26.2% at 20 h. In the early period of reaction (0–4 h),

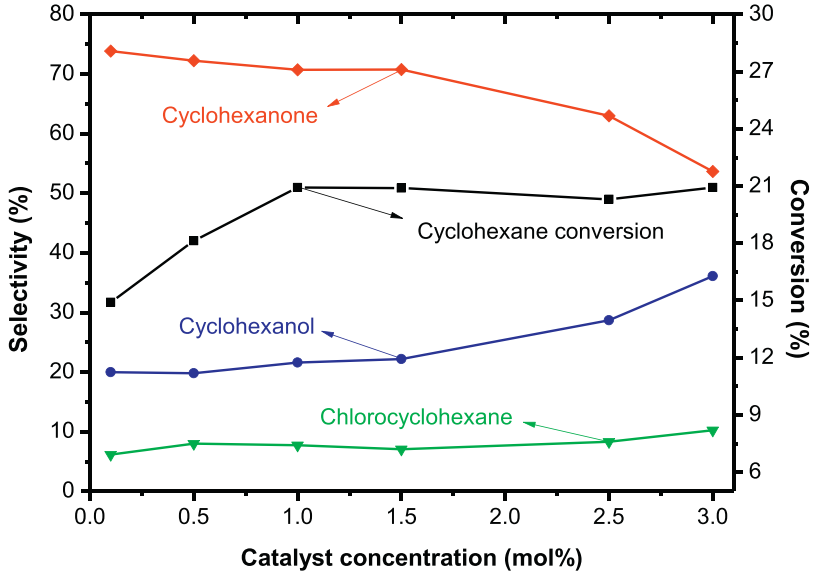

Fig. 6. Effect of the concentration of PMo_9V_3 (relative to substrate) on the photocatalytic oxidation of cyclohexane (1 mmol) by N_2O in MeCN (5.0 mL) with conc. HCl (12 M, 0.1 mL) under visible light irradiation (12 h).

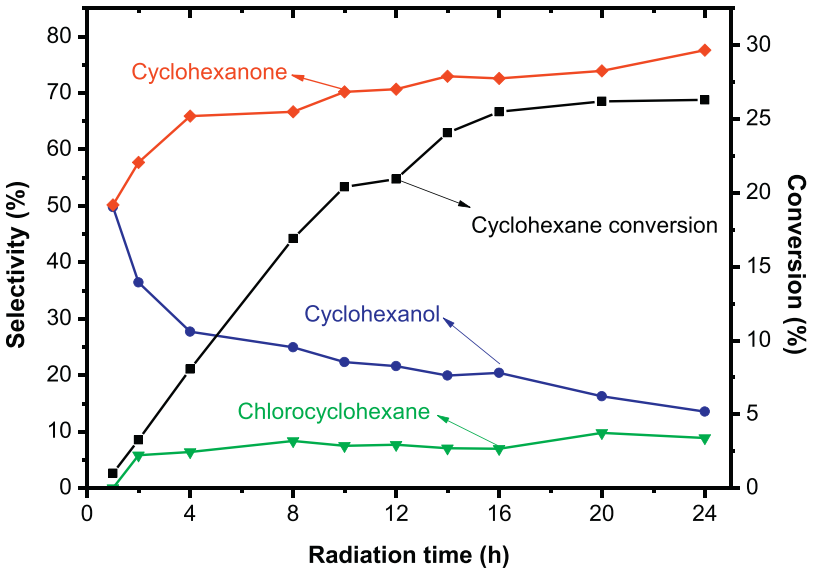

Fig. 7. Effect of irradiation time on the PMo_9V_3 (0.01 mmol, 1.96×10^{-3} M)-photocatalyzed oxidation of cyclohexane (1 mmol) by N_2O in MeCN (5.0 mL) with conc. HCl (12 M, 0.1 mL) under visible light irradiation.

cyclohexanone selectivity rapidly increased with irradiation time, along with an obvious decrease of cyclohexanol selectivity. After 4 h, its growth rate slowed down. On the whole, the influence of catalyst concentration and illumination time on the chlorination was nearly negligible in the variation range of both variables. Fig. 8 demonstrates that the amount of water added strongly affected this photocatalytic oxygenation. As water amount was increased from 0 to 0.12 mL, the conversion was continuously and slowly reduced from 22.6 to 20.0%. Further increasing the amount to 0.15 mL resulted in an obvious decrease in the conversion (14.0%). The selectivity for cyclohexanone was continuously and significantly improved from 21.8 to 82.7% with increasing water amount (from 0 to 0.15 mL), along with an obvious decrease of cyclohexanol and chlorocyclohexane. These results indicate that the additive water plays a special regulation role in this photocatalysis reaction and its adjusting mechanism will be discussed later.

3.4. Promotion mechanism of HCl aqueous solution

In order to explore the reason why the HCl aqueous solution is capable of promoting the $PMo_{12-n}V_n$ acids-catalyzed oxygenation of cyclohexane by N_2O in MeCN under visible light irradiation, we measured the UV–vis spectral changes of PMo_9V_3 acid in the present photoreaction media before and after photoreaction (see Fig. 9). As described in Fig. 2, the UV–vis spectrum of PMo_9V_3 acid in pure MeCN exhibited two characteristic LMCT bands in the 200–310 nm regions (Fig. 9a). The addition of HCl aqueous solution (and more especially dry HCl gas) to pure MeCN resulted in an obvious raising in the LMCT band near 220 nm (Fig. 9c and e), which was probably due to hydrogen bond interactions between the HCl and the Mo=O_d bonds of HPAs [52,58]. Notably, both the additives described above, especially HCl gas, led to a noticeable red-shift of the d–d transition band of PMo_9V_3 acid (see the inset

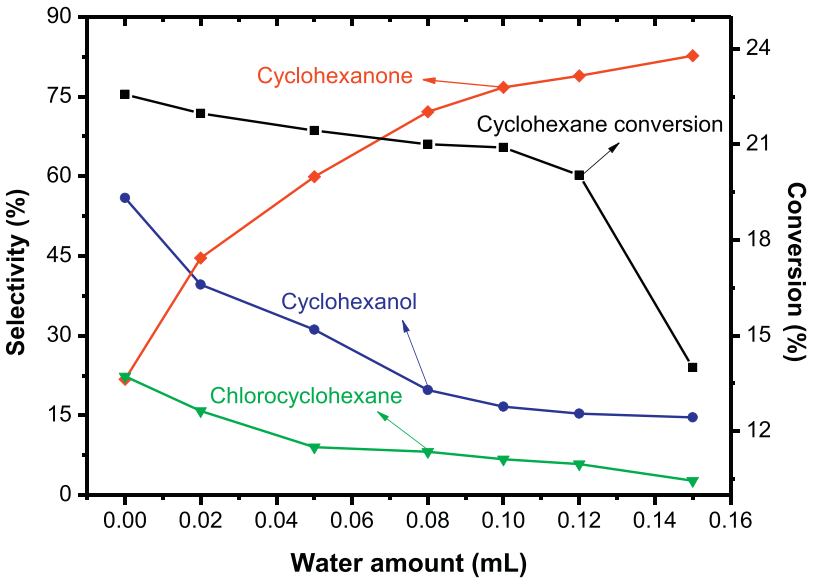

Fig. 8. Effect of water amount on the PMo_9V_3 (0.01 mmol)-photocatalyzed cyclohexane (1 mmol) oxidation by N_2O in MeCN (5.0 mL) with dry HCl gas (1.0 mmol) under visible light irradiation (12 h).

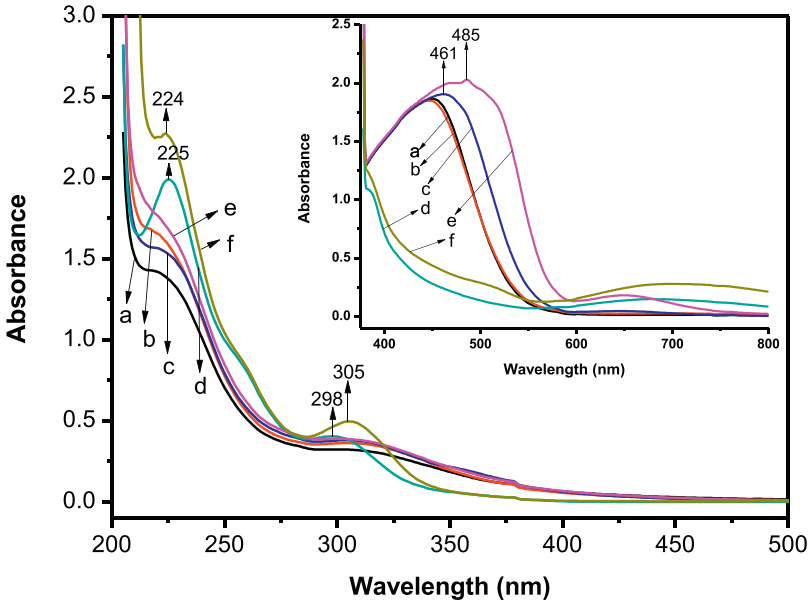

Fig. 9. The UV–vis spectra (200–500 nm) of PMo_9V_3 (1.96×10^{-5} M) in MeCN solvent with 1 mmol cyclohexane. a: The system in a pure MeCN (5.1 mL); b: after using visible light to irradiate the system a for 12 h under N_2O; c: the system in MeCN (5.0 mL) and HCl aqueous solution (12 M, 0.1 mL); d: after using visible light to irradiate the system c for 12 h under N_2O; e: the system in MeCN (5.1 mL) and HCl gas (1.2 mmol); f: after using visible light to irradiate the system e for 12 h under N_2O. Inset is the corresponding absorption spectra of PMo_9V_3 acid with high concentration (1.96×10^{-3} M) in a visible region.

in Fig. 9). At the same time, a change of the catalyst solution color from orange-yellow to orange (HCl aqueous solution) or orange-red (HCl gas) was observed in the presence of the additives (Fig. S1). These findings likely support the assertion that donor–acceptor (D–A) interactions between the coordinated metal ions of PMo_9V_3 acid and HCl lead to the formation of D–A adducts [23,32], and moreover water seems to weaken the D–A interactions. After the systems described above were illuminated by visible light for 12 h under N_2O, the changes of catalyst's UV–vis spectrum and solution color in pure MeCN were nearly negligible compared to those before light irradiation (Fig. 9b vs a and Fig. S1). An obvious increase in the two LMCT bands of PMo_9V_3 and a slight of shift in the Keggin structural band near 300 nm were, however, noticed upon the systems containing HCl aqueous solution (and more especially HCl gas) after visible light illumination (Fig. 9d vs c and f vs e). Furthermore, the intensity of the weak absorption band in 380–500 nm obviously decreased, accompanying an increase of the absorbance in 600–800 nm attributed to an intervalence charge transfer of the reduced HPAs [52,59]. The color change of catalyst solution from orange or orange-red to yellow-green was also noticed the on both systems containing the additives after visible light illumination (Fig. S1). These changes can indicate the formation of the reduced form of the catalyst.

The cyclic voltammograms (CVs) of GCE for these HPAs in various reaction media were measured in the scanning potential range of −0.4 to 1.2 V and the results are shown in Figs. 10–13 , respectively. As is shown in Fig. 10, the CV curve of PMo_{12} acid in pure MeCN exhibited four pairs of quasi-reversible redox waves at (0.034–0.269)/2 = −0.118 V, (0.302 + 0.019)/2 = 0.161 V, (0.625 + 0.283)/2 = 0.454 V and (0.869 + 0.474)/2 = 0.672 V (Fig. 10a), all of which should be assigned to the redox process between Mo^{6+} and Mo^{5+} ions [60,61]. Notably, the intensities of Mo^{6+}/Mo^{5+} redox waves of $PMo_{12-n}V_n$ were obviously weaker than those of PMo_{12} (Fig. 10b–d) as a result of the decline in acid strength [52]. On the other hand, these Mo^{6+}/Mo^{5+} redox waves gradually shifted to more negative potentials and especially the two pairs of Mo^{6+}/Mo^{5+} redox waves at higher potentials gradually merged into a single pair with increasing substituted V atom numbers (Fig. 10b–d) [60]. It is likely that the delocalization effect of the d electrons from V(V) to Mo(VI) ions, as supported by the foregoing XPS characterization, can reduce the redox prosperities of Mo^{6+}/Mo^{5+} [62]. In addition to the Mo^{6+}/Mo^{5+} redox waves described above, a pair of quasi-reversible redox waves in a higher potential region (0.6–1.1 V) was observed in the CVs of these V(V)-containing HPAs, which should be attributed to the redox process between V^{5+} and V^{4+} ions [60,63]. The oxidative and reductive potentials (E_{pa} and E_{pc}) of V^{5+}/V^{4+} redox waves over $PMo_{10}V_2$ and PMo_9V_3 acids also respectively increased and decreased compared to those over $PMo_{11}V$ acid, indicating that increasing the degree of substitution of V atoms leads to an enhancement of the oxidative capacity of HPA but a reduction of its reversibility [60].

Fig. 11 provides the CVs of these HPAs in MeCN containing HCl aqueous solution. It shows that the redox waves described above were significantly strengthened in the presence of HCl aqueous solution, which is due to an increase in the degree of ionization of these HPAs in the electrolyte HCl aqueous solution. The influence of V substitution on the Mo^{6+}/Mo^{5+} redox waves in this solution system was very similar to that in pure MeCN (Figs. 11 vs 10). Notably, the HCl aqueous solution could cause a splitting of the oxidative wave of V^{4+} to V^{5+} ions in the V(V)-substituted HPAs to become two waves, in which the more positive one was obviously strengthened from $PMo_{11}V$ to PMo_9V_3, corresponding to a gradual decrease in another one. Only a reduction wave of V^{5+} to V^{4+} ions in the range 0.5–0.6 V that likely corresponded to the oxidative wave in the range 0.6–0.7 V, however, was observed in the present conditions. This may be because the V^{5+}/V^{4+} redox waves in the higher potential region is less reversible or its reductive wave merges with another one in the range 0.5–0.6 V. It is noteworthy that adding only water to the PMo_9V_3/MeCN system could reduce the E_{pa} and E_{pc} values of the Mo^{6+}/Mo^{5+} and V^{5+}/V^{4+} redox waves, but did not result in a splitting of the oxidative wave of $V^{4+}$to V^{5+} ions (Fig. S2). According to these findings, we propose that the oxidative wave of V^{4+} to V^{5+} ions in the range 0.75–1.00 V is likely related to the adduct generated by a D–A interaction of $PMo_{12-n}V_n$ with HCl, while the another one is not. This assertion is in agreement with the results in Fig. 9 and Fig. S1 and supported by the outcomes of earlier study [61]. Furthermore, this D–A interaction is gradually strengthened on changing from $PMo_{11}V$ to PMo_3V_3, which likely

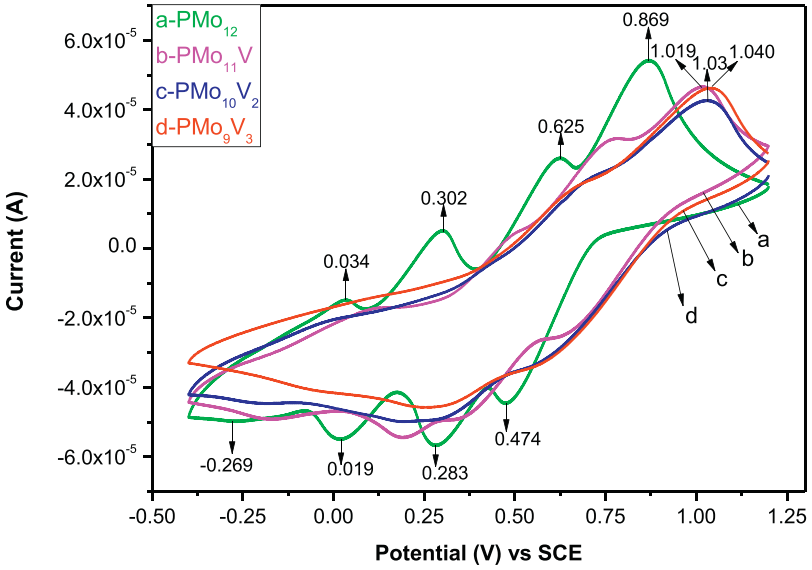

Fig. 10. Cyclic voltammograms (CVs) of PMo_{12} (a), $PMo_{11}V$ (b), $PMo_{10}V_2$ (c) and PMo_9V_3 (d) acids in pure MeCN (2.0×10^{-3} M, 10 mL).

leads to the different catalysis activity of $PMo_{12-n}V_n$ acids in the same photoreaction conditions (Table 2).

In order to further research the formation of such a D–A adduct, the effects of HCl concentration and water amount on the CVs of HPAs in HCl-MeCN solution were checked respectively by using the PMo_9V_3 acid as an example. Fig. 12 illustrates that the E_{pa} and E_{pc} values of both V^{5+}/V^{4+} and its adjacent Mo^{6+}/Mo^{5+} redox waves respectively decreased and increased, while the E_{pc} of other Mo^{6+}/Mo^{5+} waves increased more than their E_{pa} with increasing concentration of HCl. This indicates that the additive HCl gas reduces oxidative capacity of PMo_9V_3 but improves its redox reversibility. Notably, the splitting of the V^{5+}/V^{4+} oxidative wave did not occur in a low HCl concentration (0–0.06 M, Fig. 12a–c), but occurred when the concentration was enhanced to 0.10 M (Fig. 12d). Moreover, the splitting wave near 1.0 V was obviously strengthened with a slight of negative-shift upon further increasing the concentration (Fig. 12d and e). Meanwhile, a turning point appeared near the platform of cyclohexane conversion curve (Fig. 5). These observations further support that the D–A adducts between PMo_9V_3 and HCl play important roles in the photoreaction. Fig. 13 shows that when a different amount of water was introduced into the reaction system with 2.0 mmol HCl (0.20 M), the E_{pa} and E_{pc} values of V^{5+}/V^{4+} and Mo^{6+}/Mo^{5+} redox waves in the CV of PMo_9V_3 acid were gradually decreased with increasing water amount. Notably, when water amount was lower than 0.16 mL, the E_{pa} values of two oxidative waves of V^{4+} to V^{5+} ions continuously decreased but the intensities of both waves were hardly changed by the water amount. After 0.16 mL, however, the V^{4+}/V^{5+} oxidative wave assigned to the D–A adduct was gradually weakened with further increasing water amount, which is likely due to a replacement effect of an excess of H_2O on the HCl coordinated to PMo_9V_3 acid. On the other hand, the reversibility of V^{5+}/V^{4+} redox waves related to D–A adduct became obviously worse when the water amount was beyond 0.24 mL, at which came the turning point of cyclohexane conversion (Fig. 8). It is concluded from these findings that (i) the additive HCl gas or its aqueous solution can improve the reversibility of V^{5+}/V^{4+} redox waves in the V-substituted HPAs. On the other hand, the adduct generated by a D–A interaction of

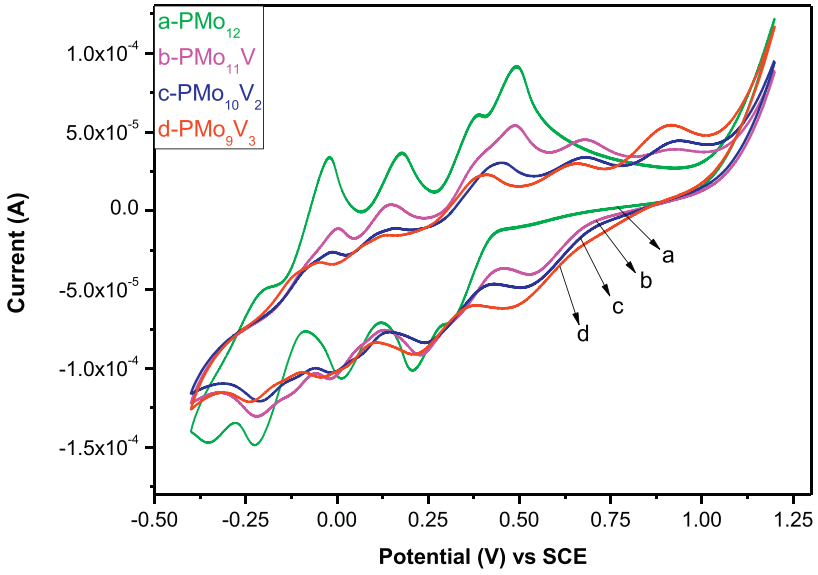

Fig. 11. Cyclic voltammograms (CVs) of PMo_{12} (a), $PMo_{11}V$ (b) $PMo_{10}V_2$ (c) and PMo_9V_3 (d) acids in MeCN (1.96×10^{-3} M, 10 mL) containing HCl (2 mmol) and H_2O (0.2 mL).

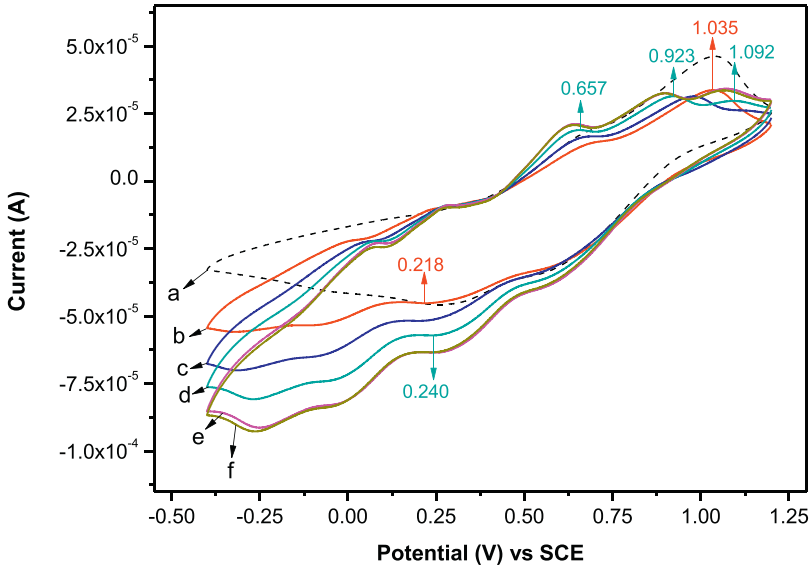

Fig. 12. Effect of HCl concentration on the cyclic voltammograms (CVs) of PMo_9V_3 in MeCN (1.96×10^{-3} M, 10 mL) with HCl gas. a: Without additive; b: adding 0.2 mmol HCl (0.02 M); c: adding 0.6 mmol HCl (0.06 M); d: adding 1.0 mmol HCl (0.10 M); e: adding 1.4 mmol HCl (0.14 M); f: adding 1.6 mmol HCl (0.16 M).

the V-substituted HPAs with HCl is likely responsible for the HCl aqueous solution-promoted photocatalytic oxidation. (ii) Adding a small amount of water to the HCl-mediated photocatalysis system slightly weakens the oxidative capacity of the V-substituted HPAs, but adding an excess amount of water will cause very unfavorable effects on the catalyst's redox reversibility and even on the formation of D-A adduct, which agrees well with the reaction results described above.

3.5. Photocatalytic mechanism

Photocatalytic decomposition of N_2O usually needs UV light to proceed at room temperature [1]. In addition, allowing for the fact that N_2O is generally considered to be inert in kinetics [38] and a poor ligand to transition metals [39], the initiation of chain reaction by direct activation of HCl rather than N_2O is preferable. A reasonable reaction mechanism is hence proposed as follows (using the PMo_9V_3 catalysis system as an example, Scheme 2). Firstly, a $[PMo_9V^V{}_3O_{40}]^{6-}$ anion can react with a HCl to form a donor–acceptor (D–A) adduct $[PMo_9V^V{}_3O_{40}{}^{6-}\text{-HCl}]$ (Eq. (1)). It is most likely that such an adduct is excited by visible light to realize the single electron transfer from its Cl^- to the V^{5+} ions, which can lead to the formation of its reduced form ($[PMo_9V^V{}_2V^{IV}O_{40}]^{7-}$) and a Cl radical ($Cl^\bullet$) (Eq. (2)). Next, the $Cl^\bullet$ easily abstracts one H atom from cyclohexane to form a HCl and cyclohexyl radical ($Cy^\bullet$, Eq. (3)) [45,64]. The $Cy^\bullet$ may react with the N_2O pre-activated by the reduced form $[PMo_9V^V{}_2V^{IV}O_{40}]^{7-}$ as an electron donor to form an unstable radical adduct, and then the adduct is rapidly decomposed to generate a cyclohexoxy radical ($CyO^\bullet$), along with nitrogen (N_2) evolution (Eq. (4)). This pre-activation effect may derive from the D–A interaction between N_2O and PMo_9V_3 acid [23,32]. Also, a similar activation pathway for the addition of N_2O

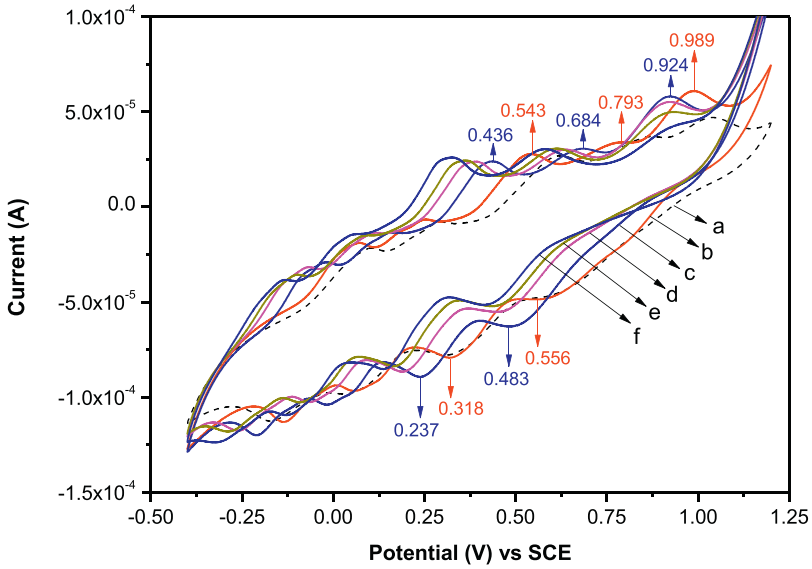

Fig. 13. Effect of water on the cyclic voltammograms (CVs) of PMo_9V_3 (0.02 mmol) in MeCN (10 mL) containing HCl gas (2.0 mmol, 0.2 M). a: Without H_2O; b: adding 0.04 mL H_2O; c: adding 0.16 mL H_2O; d: adding 0.24 mL H_2O; e: adding 0.3 mL H_2O; f: adding 0.40 mL H_2O.

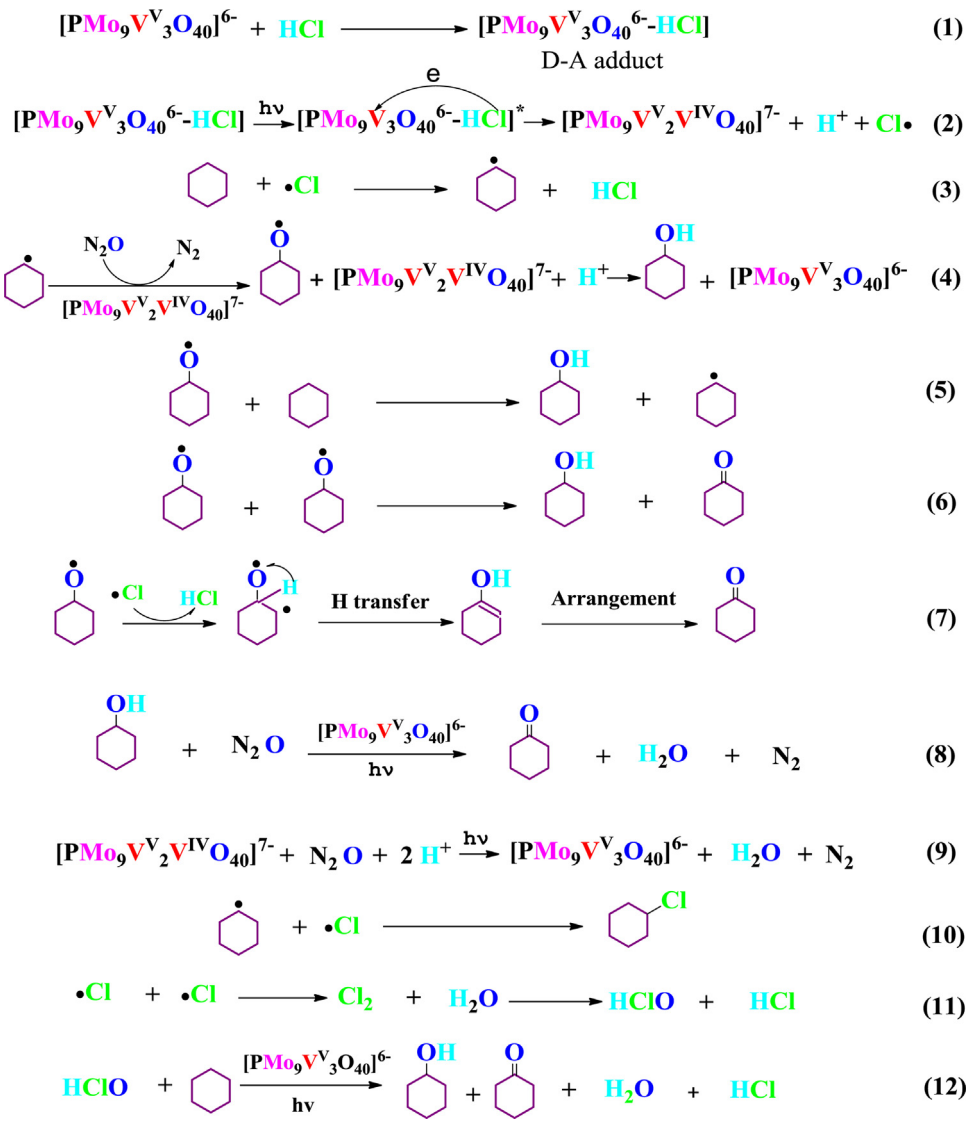

Scheme 2. Proposed photocatalytic mechanism.

with alkyl radicals has been reported by Ohtani and co-workers in the Pt particles-catalyzed selective oxidation of alcohols, ethers and amines by N_2O [65]. The CyO• can be converted to cyclohexanol (CyOH) through the following pathways: (i) the reduced state $[PMo_9V^V_2V^{IV}O_{40}]^{7-}$ is oxidized by it to regenerate the original $[PMo_9V^V_3O_{40}]^{6-}$ with the participation of H^+ (i.e., catalytic cycle pathway, Eq. (4)), in agreement with catalyst's concentration effect (Fig. 6), since the negative charge accumulation near the O = VO_4 moiety of $[PMo_9V^V_2V^{IV}O_{40}]^{7-}$ can attract and bind the organic radical cation [66]; (ii) it abstracts one H atom of cyclohexane to give a CyOH and another Cy• radical (i.e., an auto-oxidation pathway, Eq. (5)) [67]. The following three reactions likely result in the formation of cyclohexanone (Cy = O): (i) the H transfer reaction between two CyO• radicals can produce an equivalence of Cy = O and CyOH (Eq. (6)) [68]; (ii) the Cl• further removes one H atom from the adjacent carbon of CyO• to give an unstable biradical, and then the latter can be converted to Cy = O *via* a H transfer from carbon to oxygen followed by enol rearrangement (Eq. (7)); (iii) the CyOH is further oxidized by N_2O to Cy = O upon photocatalysis with the $[PMo_9V^V_3O_{40}]^{6-}$ anion (Eq. (8)) though it is not the dominant reaction pathway to produce Cy = O (Table 2, Entry 15). Considering that the accumulation of CyOH was only a little under optimized conditions (Fig. 8), another pathway that the reduced catalyst is directly oxidized by N_2O likely exists (Eq. (9)) in order to complete catalytic cycle efficiently. Noteworthily, this pathway can hardly proceed in present system without irradiation, as supported by Figs. S3 and S4. We hence propose that this pathway likely needs visible light irradiation, seeing that the visible light-excited Keggin-type heteropoly blue (HPB) can serve as a strong electron donor [69,70] and moreover the reduction of N_2O is thermodynamically favorable in a protic medium [1]. Undoubtedly, the combination of Cy• with Cl• radicals easily leads to the formation of chlorocyclohexane (Eq. (10)). The improved effect of water on the selectivity of KA oil (and especially cyclohexanone) in the present photoreaction system may be due to the following reasons. (i) Adding a suitable amount of water, as supported by the above CV measurements, can slightly weaken the oxidative capacity of the V(V)-containing HPAs, thus slowing down the formation of Cl• radicals. As a result, a good match in rate is easily realized among the reactions described above in Eqs. (1)–(8), which easily leads to improving the KA oil selectivity. (ii) A stabilization effect of water on the intermediates CyO• radicals is perhaps favorable to the promotion of the reaction in Eq. (7) by reducing the impact of solvent (MeCN) cage effect which benefits the formation of cyclohexanol (Eqs. (4)–(6)). (iii) The Cl_2 formed *via* the combination of two Cl• radicals easily reacts with water to generate a HClO (Eq. (11)) and the latter, as an oxidant,

may play a positive role in improving the selectivity of the KA oil (Eq. (12)).

4. Conclusion

In summary, for the first time we have developed a mild and efficient method to synthesize cyclohexane-derived KA oil using N_2O as an oxidant, which is catalyzed by the V(V)-substituted molybdophosphoric acids under visible light irradiation in the presence of HCl aqueous solution. The newly-developed catalytic system has the following advantages: (i) the photocatalyst and light source used in the present system are cheap and easily obtained; (ii) using N_2O as an oxidant is of both environmental and economic significances in its recycling and the production of adipic acid, and (iii) very moderate operating conditions, high photocatalytic efficiency and good selectivity for KA oil (especially cyclohexanone) under optimized conditions. The cooperation mechanism between the excited state of catalyst and that of its reduced form (heteropoly blue, HPB) is likely responsible for the reaction performances. D–A interactions play important roles in this catalytic system, whatever in the chain initiation or the regulation of catalyst's redox property. Moreover, the D–A interaction between HPB and N_2O may give assistance to the activation of N_2O. Hence we are interested in further exploiting the D–A interaction of HPAs with HCl (and more especially with N_2O) to develop more efficient HPA photocatalysis system for selective oxidation of cyclohexane and other organic compounds to the corresponding oxygenated products by N_2O.

Acknowledgments

We acknowledge the financial support for this work by the Specialized Research Fund for the Doctoral Program of Higher Education (20124306110005, 20120010110003), the National Natural Science Fund of China (20873040, 21203060), the Natural Science Fund of Hunan Province (10JJ2007, 14JJ2148), the Innovation Platform Open Fund of Hunan College (11K044), the Program for Science and Technology Innovative Research Team in Higher Educational Institutions of Hunan Province, the 100 Talents Program of Hunan Province and the Hunan Provincial Innovation Foundation for Postgraduate of China (CX2013B207).

Appendix A. Supplementary data

Supplementary data associated with this article can be found, in the online version, at http://dx.doi.org/10.1016/j.apcatb.2015.09.048.

References

[1] A.V. Leont'ev, O.A. Fomicheva, M.V. Proskurnina, N.S. Zefirov, Russ Chem. Rev. 70 (2001) 91–104.
[2] J. Pérez-Ramírez, F. Kapteijn, K. Schöffel, J.A. Moulijn, Appl. Catal. B: Environ. 44 (2003) 117–151.
[3] S. Van de Vyver, Y. Román-Leshkov, Catal. Sci. Technol. 3 (2013) 1465–1479.
[4] F. Kapteijn, J. Rodriguez-Mirasol, J.A. Moulijn, Appl. Catal. B: Environ. 9 (1996) 25–64.
[5] A. Shimizu, K. Tanaka, M. Fujimori, Chemosphere Global Change Sci. 2 (2000) 425–434.
[6] J.A.Z. Pieterse, G.D. Pirngruber, J.A. van Bokhoven, S. Booneveld, Appl. Catal. B: Environ. 71 (2007) 16–22.
[7] M.C. Campa, V. Indovina, D. Pietrogiacomi, Appl. Catal. B: Environ. 91 (2009) 347–354.
[8] P. Sazama, B. Wichterlová, E. Tábor, P. Šťastný, N.K. Sathu, Z. Sobalík, J. Dědeček, P. Sklenák, A. Vondrová, J. Catal. 312 (2014) 123–138.
[9] B. Coq, M. Mauvezin, G. Delahay, S. Kieger, J. Catal. 195 (2000) 298–303.
[10] J. Pérez-Ramírez, F. Kapteijn, Appl. Catal. B: Environ. 47 (2004) 177–187.
[11] K. Sugawara, T. Nobukawa, M. Yoshida, Y. Sato, K. Okumura, K. Tomishige, K. Kunimori, Appl. Catal. B: Environ. 69 (2007) 154–163.
[12] M. Konsolakis, C. Drosou, I.V. Yentekakis, Appl. Catal. B: Environ. 123–124 (2012) 405–413.
[13] D.P. Ivanov, V.I. Sobolev, L.V. Pirutko, G.I. Panov, Adv. Synth. Catal. 344 (2002) 986–995.
[14] P. Kuśtrowski, L. Chmielarz, J. Surman, E. Bidzińska, R. Dziembaj, P. Cool, E.F. Vansant, J. Phys. Chem. A 109 (2005) 9808–9815.
[15] T. Thömmes, S. Zürcher, A. Wix, A. Reitzmann, B. Kraushaar-Czarnetzki, Appl. Catal. A: Gen. 318 (2007) 160–169.
[16] B.P.C. Hereijgers, B.M. Weckhuysen, J. Catal. 270 (2010) 16–25.
[17] H. Yu, F. Peng, J. Tan, X.W. Hu, H.J. Wang, J. Yang, W.X. Zheng, Angew. Chem. Int. Ed. 50 (2011) 3978–3982.
[18] W.F. Wu, Z.H. Fu, S.P. Tang, S. Zou, X. Wen, Y. Meng, S.B. Sun, J. Deng, Y.C. Liu, D.L. Yin, Appl. Catal. B: Environ. 164 (2015) 113–119.
[19] F. Cavani, S. Alini, in: F. Cavani, G. Centi, S. Perathoner, F. Trifiró (Eds.), Sustainable Industrial Chemistry, Wiley-VCH, Weinheim, 2009, pp. 367–425.
[20] V. Hessel, I. Vural Gürsel, Q. Wang, T. Noël, J. Lang, Chem. Eng. Technol. 35 (2012) 1184–1204.
[21] V.N. Parmon, G.I. Panov, A. Uriarte, A.S. Noskov, Catal. Today 100 (2005) 115–131.
[22] M. Sun, J.Z. Zhang, P. Putaj, V. Caps, F. Lefebvre, J. Pelletier, J.M. Basset, Chem. Rev. 114 (2014) 981–1019.
[23] R. Ben-Daniel, R. Neumann, Angew. Chem. Int. Ed. 42 (2003) 92–95.
[24] S. Gopalakrishnan, A. Zampieri, W. Schwieger, J. Catal. 260 (2008) 193–197.
[25] L.V. Pirutko, V.S. Chernyavsky, E.V. Starokon, A.A. Ivanov, A.S. Kharitonov, G.I. Panov, Appl. Catal. B: Environ. 91 (2009) 174–179.
[26] P.J. Smeets, J.S. Woertink, B.F. Sels, E.I. Solomon, R.A. Schoonheydt, Inorg. Chem. 49 (2010) 3573–3583.
[27] G.N. Li, E.A. Pidko, R.A. van Santen, Z.C. Feng, C. Li, E.J.M. Hensen, J. Catal. 284 (2011) 194–206.
[28] A.J.J. Koekkoek, W. Kim, V. Degirmenci, H. Xin, R. Ryoo, E.J.M. Hensen, J. Catal. 299 (2013) 81–89.
[29] M. Guisnet, F.R. Ribeiro, Deactivation and Regeneration of Zeolite Catalysts, Imperial College Press, London, 2011.
[30] S. Gopalakrishnan, S. Yada, J. Muench, T. Selvam, W. Schwieger, M. Sommer, W. Peukert, Appl. Catal. A: Gen. 327 (2007) 132–138.
[31] T. Thömmes, I. Gräf, A. Reitzmann, B. Kraushaar-Czarnetzki, Ind. Eng. Chem. Res. 49 (2010) 2624–2637.
[32] R. Ben-Daniel, L. Weiner, R. Neumann, J. Am. Chem. Soc. 124 (2002) 8788–8789.
[33] L.J. Csányi, K. Jáky, J.T. Kiss, I. Ilisz, P. Forgó, G. Dombi, J. Mol. Catal. A: Chem. 263 (2007) 48–54.
[34] J. Ettedgui, R. Neumann, J. Am. Chem. Soc. 131 (2009) 4–5.
[35] E.K. Beloglazkina, A.G. Majouga, A.A. Moiseeva, N.V. Zyk, Phosphorus Sulfur Silicon 188 (2013) 377–383.
[36] G. Kiefer, L. Jeanbourquin, K. Severin, Angew. Chem. Int. Ed. 52 (2013) 6302–6305.
[37] S. Saito, H. Ohtake, N. Umezawa, Y. Kobayashi, N. Kato, M. Hirobe, T. Higuchi, Chem. Commun. 49 (2013) 8979–8981.
[38] R.G.S. Banks, R.J. Henderson, J.M. Pratt, J, Chem. Soc. A 288 (1968) 2886–2889.
[39] F. Bottomley, I.J.B. Lin, M. Mukaida, J. Am. Chem. Soc. 102 (1980) 5238–5242.
[40] I.V. Kozhevnikov, Chem. Rev. 98 (1998) 171–198.
[41] S. Yamaguchi, S. Sumimoto, Y. Ichihashi, S. Nishiyama, S. Tsuruya, Ind. Eng. Chem. Res. 44 (2005) 1–7.
[42] R. Neumann, A.M. Khenkin, Chem. Commun. (2006) 2529–2538.
[43] A. Troupis, T.M. Triantis, E. Gkika, A. Hiskia, E. Papaconstantinou, Appl. Catal. B: Environ. 86 (2009) 98–107.
[44] J. Zhang, Y. Tang, Q. Luo, M. Jian, C.W. Hu, Chinese J. Inorg. Chem. 20 (2004) 935–940.
[45] W.F. Wu, X.L. He, Z.F. Fu, Y.C. Liu, Y.L. Wang, X.L. Gong, X.L. Deng, H.T. Wu, Y.H. Zou, N.Y. Yu, D.L. Yin, J. Catal. 286 (2012) 6–12.
[46] G.A. Tsigdinos, C.J. Hallada, Inorg. Chem. 7 (1968) 437–441.
[47] D. Casarini, G. Centi, P. Jiru, V. Lena, Z. Tvaruzkova, J. Catal. 143 (1993) 325–344.
[48] C. Rocchiccioli-Deltcheff, M. Fournier, J. Chem. Soc., Faraday Trans. 87 (1991) 3913–3920.
[49] A. Brückner, G. Scholz, D. Heidemann, M. Schneider, D. Herein, U. Bentrup, M. Kant, J. Catal. 245 (2007) 369–380.
[50] T. Ilkenhans, B. Herzog, T. Braun, R. Schlögl, J. Catal. 153 (1995) 275–292.
[51] N.A. Alekar, S.B. Halligudi, R. Rajani, S. Gopinathan, C. Gopinathan, React. Kinet. Catal. Lett. 72 (2001) 169–176.
[52] E.B. Wang, C.W. Hu, L. Xu, Introduction of Polyacids Chemistry, Chemical Industry Press, Beijing, 1998.
[53] S. Damyanova, J.L.G. Fierro, I. Sobrados, J. Sanz, Langmuir 15 (1990) 469–476.
[54] D. Barats-Damatov, L.J.W. Shimon, Y. Feldman, T. Bendikov, R. Neumann, Inorg. Chem. 54 (2015) 628–634.
[55] C.D. Wagner, W.M. Riggs, L.E. Davis, J.F. Moulder, G.E. Mullenberg, Handbook of X-ray Photoelectron Spectroscopy, Perkin-Elmer Corporation, Eden Prairie, 1979.
[56] P. Delichere, K.E. Bere, M. Abon, Appl. Catal. A 172 (1998) 295–309.
[57] B. Herzog, W. Bensch, T. Ilkenhans, R. Schlögl, Catal. Lett. 20 (1993) 203–219.
[58] A.J. Esswein, D.G. Nocera, Chem. Rev. 107 (2007) 4022–4047.
[59] K. Malka, J. Aubard, M. Delamar, V. Vivier, M. Che, C. Louis, J. Phys. Chem. B 107 (2003) 10494–10505.
[60] S.B. Jing, H.B. Zhang, W.C. Zhu, Z.L. Wang, G.J. Wang, J. Jilin Univ. (Sci. Ed.) 41 (2003) 534–537.
[61] E. Itabashi, Bull. Chem. Soc. Jpn. 60 (1987) 1333–1336.
[62] J.M. Maestre, X. Lopez, C. Bo, J.M. Poblet, N. Casañ-Pastor, J. Am. Chem. Soc. 123 (2001) 3749–3758.

[63] S. Himeno, N. Ishio, J. Electroanal. Chem. 451 (1998) 203–209.
[64] J. Platz, J. Sehested, O.J. Nielsen, J. Phys. Chem. A 103 (1999) 2688–2695.
[65] B. Ohtani, S. Takamiya, Y. Hirai, M. Sudoh, S. Nishimoto, T. Kagiya, J. Chem. Soc., Perkin Trans. II 2 (1992) 175–179.
[66] H. Hirao, D. Kumar, H. Chen, R. Neumann, S. Shaik, J. Phys. Chem. C 111 (2007) 7711–7719.
[67] I. Hermans, J. Peeters, P.A. Jacobs, J. Phys. Chem. A 112 (2008) 1747–1753.
[68] R. Lee, L.F. Albright, Ind. Eng. Chem. Proc. Des. Dev. 4 (1965) 411–420.
[69] M. Yoon, J.A. Chang, Y. Kim, J.R. Choi, K. Kim, S.J. Lee, J. Phys. Chem. B 105 (2001) 2539–2545.
[70] N. Fu, G.X. Lu, Appl. Surf. Sci. 255 (2009) 4378–4383.